

Experimental test of nonlocal realism using a fiber-based source of polarization-entangled photon pairs

M. D. Eisaman,¹ E. A. Goldschmidt,¹ J. Chen,² J. Fan,^{1,*} and A. Migdall¹

¹*Optical Technology Division, National Institute of Standards and Technology, 100 Bureau Drive, Mail Stop 8441, Gaithersburg, Maryland 20899-8441, USA and Joint Quantum Institute, University of Maryland, College Park, Maryland 20742, USA*

²*Institute of Computational Mathematics and Applied Physics, P.O. Box 8009 (28), 100088 Beijing, People's Republic of China*

(Received 14 September 2007; published 25 March 2008)

We describe an experimental test of local realistic and nonlocal realistic theories using polarization-entangled two-photon singlet states created using a fiber-based polarization Sagnac interferometer. We show a violation of Bell's inequality in the Clauser-Horne-Shimony-Holt form by 15 standard deviations, thus excluding local hidden-variable theories, and a violation of a Leggett-type nonlocal hidden-variable inequality by more than three standard deviations, thus excluding a class of nonlocal hidden-variable theories.

DOI: [10.1103/PhysRevA.77.032339](https://doi.org/10.1103/PhysRevA.77.032339)

PACS number(s): 03.67.Mn, 03.65.Ud, 42.65.Lm, 42.50.Dv

Quantum theory confounds our conventional perceptions of locality (events in spacelike separated regions cannot affect each other) and realism (the idea that an external reality exists independent of observation). Entanglement [1], for example, which lies at the heart of quantum theory, connects two polarization-entangled photons such that by measuring the polarization of photon 1, the polarization information of photon 2 is immediately determined, even when these two photons are spacelike separated. This behavior, which Einstein referred to as “spukhafte Fernwirkungen,” or “spooky action at a distance” [2], runs counter to our everyday experience with locality and realism. Locality demands the conservation of causality, meaning that information cannot be exchanged between two spacelike separated parties or actions, while realism requires that physical observations are properties possessed by the system whether observed or not. Quantum theory offers only probabilistic explanations to physical observations. Hidden-variable theories are an attempt to complete this description in the sense described by Einstein, Podolsky, and Rosen [3].

In local hidden-variable (LHV) theories, the quantum state of a physical system is completely characterized by a unique set of hidden variables (λ) and a system-defined distribution function $\rho(\lambda)$. In the case where photon polarization is the observable of interest, the expectation value of the polarization observable (A) on photon 1 is given as $\bar{A} = \int_{\lambda} A(\lambda) \rho(\lambda) d\lambda$, which is independent of the same measurement conducted on photon 2, $\bar{B} = \int_{\lambda} B(\lambda) \rho(\lambda) d\lambda$, and vice versa. The joint property \overline{AB} is simply a statistical average with $\overline{AB} = \int_{\lambda} A(\lambda) B(\lambda) \rho(\lambda) d\lambda$.

Even without assuming explicit forms of the hidden variables and their distribution functions, it is possible to make experimentally testable predictions with LHV theories. The most famous prediction is Bell's theorem [4], which proves that the predictions of quantum mechanics do not agree with local realistic theories. Experimental investigations of Bell's theorem typically test the Clauser, Horne, Shimony, and Holt (CHSH) form of Bell's inequality [5]. The violation of this

inequality has been consistently reported in many experiments, therefore invalidating LHV theories [6]. This violation of local realism requires that we must abandon either locality or realism, if not both, but tests of the CHSH inequality do not tell us which to abandon.

In going beyond LHV theories, Leggett defined a class of nonlocal hidden variable (NLHV) theories [7]. For the class of NLHV theories, expectation values of observables depend on the orientations of polarization analyzers \vec{a} (in detecting photon 1 which has polarization \vec{u}) and \vec{b} (in detecting photon 2 which has polarization \vec{v}), $\bar{A}(\vec{u}) = \int_{\lambda} d\lambda \rho_{\vec{u},\vec{v}}(\lambda) A(\vec{a}, \vec{b}, \lambda) = \vec{u} \cdot \vec{a}$, $\bar{B}(\vec{v}) = \int_{\lambda} d\lambda \rho_{\vec{u},\vec{v}}(\lambda) B(\vec{a}, \vec{b}, \lambda) = \vec{v} \cdot \vec{b}$, and $\overline{AB}(\vec{u}, \vec{v}) = \int_{\lambda} d\lambda A(\vec{a}, \vec{b}, \lambda) B(\vec{a}, \vec{b}, \lambda) \rho_{\vec{u},\vec{v}}(\lambda)$, where $\rho_{\vec{u},\vec{v}}(\lambda)$ is the distribution function in the subensemble space spanned by photon 1 and photon 2 of different hidden variables. The joint property is averaged over all subensemble spaces, $\langle \overline{AB} \rangle = \int \int_{\vec{u},\vec{v}} d\vec{u} d\vec{v} F(\vec{u}, \vec{v}) \overline{AB}(\vec{u}, \vec{v})$, where, $F(\vec{u}, \vec{v})$ is the distribution function and $\int_{\lambda} d\lambda \rho_{\vec{u},\vec{v}}(\lambda) = \int \int_{\vec{u},\vec{v}} d\vec{u} d\vec{v} F(\vec{u}, \vec{v}) = 1$. Leggett theoretically proved that the prediction of this class of NLHV theories is incompatible with quantum theory, based on which, Gröblacher *et al.* further introduced a Leggett-type NLHV inequality to make this class of NLHV theories experimentally testable using polarization-entangled photon-pairs [8] that have become available in many research laboratories [9–11].

The introduced Leggett-type NLHV inequality [8] is expressed as

$$S_{\text{NLHV}} = |E_{11}(\phi) + E_{23}(0)| + |E_{22}(\phi) + E_{23}(0)| \leq 4 - \frac{4}{\pi} \left| \sin \frac{\phi}{2} \right|, \quad (1)$$

where $E_{11}(\phi)$, $E_{23}(0)$, and $E_{22}(\phi)$ are given as

$$E_{ij} = \frac{C_{ij} + C_{i^{\perp}j^{\perp}} - C_{ij^{\perp}} - C_{i^{\perp}j}}{C_{ij} + C_{i^{\perp}j^{\perp}} + C_{ij^{\perp}} + C_{i^{\perp}j}}$$

C_{ij} is the joint correlation measurement, $C_{ij} = \int \int_{\vec{u},\vec{v},\lambda} d\vec{u} d\vec{v} d\lambda F(\vec{u}, \vec{v}) A(\vec{a}_i, \vec{b}_j, \lambda) B(\vec{a}_i, \vec{b}_j, \lambda) \rho(\vec{u}, \vec{v})$, with $A(\vec{a}_i, \vec{b}_j, \lambda) = +1 [B(\vec{a}_i, \vec{b}_j, \lambda) = +1]$ for detecting a photon 1

*jfan@nist.gov

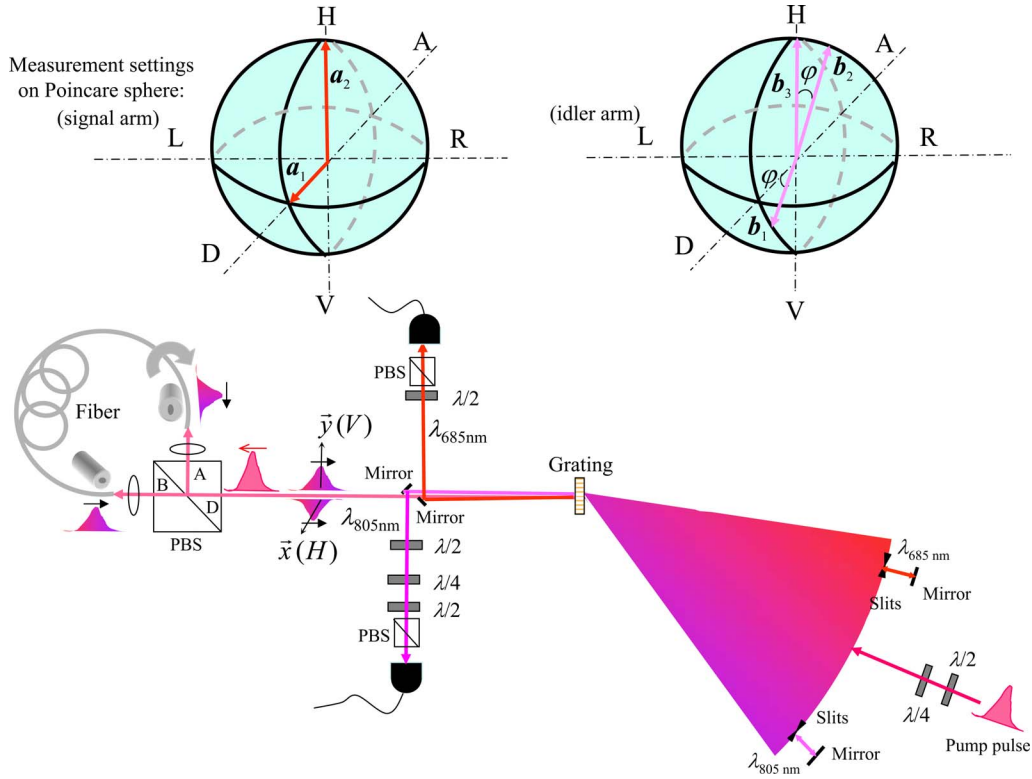


FIG. 1. (Color online) Top: Poincaré spheres showing the polarization analyzer settings in detecting the signal (left) and idler (right) photons. Bottom: Schematic of the experimental setup. Fiber: polarization-maintaining microstructure fiber, PBS: polarizing beam splitter, $\lambda/2$: half-wave plate, $\lambda/4$: quarter-wave plate, M: mirror, and IF: interference filter. The Sagnac interferometer outputs Bell states in the form of $H_{\text{signal}}H_{\text{idler}} - V_{\text{signal}}V_{\text{idler}}$, which are rotated to be the singlet state $\Psi^- = H_{\text{signal}}V_{\text{idler}} - V_{\text{signal}}H_{\text{idler}}$ by the first half-wave plate in the idler arm.

[2] and $A(\vec{a}_i, \vec{b}_j, \lambda) = -1$ [$B(\vec{a}_i, \vec{b}_j, \lambda) = -1$] for not detecting a photon 1 (2). The subscripts i, j, i^\perp , and j^\perp correspond to polarization analyzer settings with orientations along $\vec{a}_i, \vec{b}_j, \vec{a}_i^\perp$ (orthogonal to \vec{a}_i), and \vec{b}_j^\perp (orthogonal to \vec{b}_j), respectively.

As shown in Fig. 1, with orientations of polarization analyzers chosen to have the plane $(\vec{a}_1 \times \vec{b}_1)$ orthogonal to the plane $(\vec{a}_2 \times \vec{b}_2)$ in the Poincaré sphere, and $\vec{a}_2 = \vec{b}_3$, at $\varphi = 18.8^\circ$ ($\sin \varphi = \frac{|\vec{a}_1 \times \vec{b}_1|}{|\vec{a}_1||\vec{b}_1|} = \frac{|\vec{a}_2 \times \vec{b}_2|}{|\vec{a}_2||\vec{b}_2|}$), quantum theory predicts $S_{\text{NLHV}} = 2(1 + \cos \varphi) = 3.893$ for polarization-entangled photon pairs of singlet, while the class of NLHV theories to be examined gives a bound of 3.792, resulting in the maximal violation of the inequality, thus excluding a class of NLHV theories [8]. In the meantime, the Bells' inequality can be examined in the form of

$$S_{\text{CHSH}} = |E_{11}(\varphi) + E_{12}(\varphi) + E_{21}(\varphi) - E_{22}(\varphi)| \leq 2. \quad (2)$$

At $\varphi = 18.8^\circ$, quantum theory predicts $S_{\text{CHSH}} = 2 \cos \varphi + \sin \varphi = 2.215$, while the LHV limit is 2 at all angles, thus simultaneously invalidating the LHV theories.

In addition to the derivation of Leggett type of NLHV inequality, Gröblacher *et al.* conducted the first experiment to show the violation of this inequality using polarization-entangled photon pairs created via the parametric down conversion process, a $\chi^{(2)}$ nonlinear process [8]. In this paper, we examine Bell's inequality and the Leggett type of NLHV

inequality using a polarization-entangled two-photon singlet state [$\psi^- = \frac{1}{\sqrt{2}}(H_1V_2 - V_1H_1)$, where $H_i(V_j)$ means that photon i (j) is horizontally (vertically) polarized] emitted from a single-mode optical-fiber source that uses the $\chi^{(3)}$ nonlinear process of four-wave mixing to produce the photons. We show the simultaneous violations of these two inequalities by 15 and 3 standard deviations, respectively, thus excluding LHV and a certain class of NLHV theories using a source of this type.

The fiber-based source of polarization-entangled photon pairs is realized by bidirectionally pumping a polarization Sagnac interferometer (see Fig. 1), which is constructed with a polarizing beam splitter (PBS) and a 1.8 m polarization-maintaining microstructure fiber with large $\chi^{(3)}$ nonlinearity (zero-dispersion wavelength $\lambda_{\text{zdw}} = 745 \pm 5$ nm, nonlinearity $\gamma = 70 \text{ W}^{-1} \text{ km}^{-1}$ at λ_p), and with its principal axis twisted by 90° from end to end. Two identical pump pulses (8 ps, $\lambda_p = 740.7$ nm, repetition rate = 76 MHz) counterpropagate along the fiber with each creating biphoton states over a broad spectral range via a four-wave mixing process. The twisted fiber configuration allows the biphoton states from the two four-wave mixing processes which are cross-polarized with respect to each other overlap at the PBS, forming polarization-entangled photon pairs over a broad spectral range. Then a two-pass grating configuration is introduced to select output polarization-entangled photon pairs at various sets of signal and idler wavelengths ($\omega_{\text{signal}} + \omega_{\text{idler}} = 2\omega_p$) in single-spatial modes with a collection

TABLE I. Summary of nonlocality and realism tests measured for two sets of wavelengths. The particular inequality parameters and their violations were extracted from the indicated sets of correlation coefficients. All measurements taken at $\varphi=20^\circ$ with a 5-s collection time for each coincidence measurement. Visibilities ($V_{D/A}$, $V_{L/R}$, and $V_{H/V}$ are measured in diagonal-, circular-, and horizontal-vertical-polarization bases, respectively) are after subtracting the background coincidences and all uncertainties are the standard deviation of the mean. Violations for S_{NLHV} (S_{CHSH}) are calculated by subtracting the classical limit for $\varphi=20^\circ$ of 3.7789 (2.0) from the measured value of S_{NLHV} (S_{CHSH}), and dividing this by the calculated standard deviation.

λ_{signal} (nm)	λ_{idler} (nm)	Visibilities (%)	Correlation coefficients	Inequality parameter	Violation
685	805	$V_{D/A}=98.5 \pm 0.8$ $V_{R/L}=97.5 \pm 0.8$ $V_{H/V}=98.6 \pm 0.7$	$E_{23}=-0.9886 \pm 0.0071$	$S_{\text{NLHV}}=3.824 \pm 0.014$ $S_{\text{CHSH}}=2.176 \pm 0.013$	3.2σ 14σ
			$E_{11}=-0.8776 \pm 0.0066$		
			$E_{22}=-0.9689 \pm 0.0074$		
			$E_{12}=0.0637 \pm 0.0055$		
			$E_{21}=0.3935 \pm 0.0051$		
689	800	$V_{D/A}=99.0 \pm 0.8$ $V_{R/L}=98.0 \pm 0.8$ $V_{H/V}=99.0 \pm 0.7$	$E_{23}=-0.9902 \pm 0.0076$	$S_{\text{NLHV}}=3.831 \pm 0.015$ $S_{\text{CHSH}}=2.205 \pm 0.012$	3.4σ 17σ
			$E_{11}=-0.8949 \pm 0.0075$		
			$E_{22}=-0.9557 \pm 0.0081$		
			$E_{12}=0.0555 \pm 0.0060$		
			$E_{21}=0.3886 \pm 0.0056$		

bandwidth of $\Delta\lambda=0.9$ nm. With appropriate phase-control of the pump beam [11], the Sagnac interferometer outputs Bell's state, $\Phi^- = \frac{1}{\sqrt{2}}(H_{\text{signal}}H_{\text{idler}} - V_{\text{signal}}V_{\text{idler}})$. By inserting a half-wave plate into the beam path of the idler photon, we produce the singlet state $\Psi^- = \frac{1}{\sqrt{2}}(H_{\text{signal}}V_{\text{idler}} - V_{\text{signal}}H_{\text{idler}})$. Previous work in our laboratory has shown the robust phase-stability, high spectral brightness, and single-spatial-mode feature of this fiber-based source [12]. We also used this source to demonstrate the violation of Bell's inequality for all four Bell states by at least 22σ (standard deviation) for wavelengths over a 15 nm range [13].

Considering the rotational symmetry of the singlet state, the correlation measurement C_{ij} can be obtained from two-photon coincidence events counted for a few groups of polarization analyzer settings. Following the experimental scheme proposed by Gröblacher *et al.* [8], the orientations of the polarization analyzers are chosen to have \vec{a}_1 and \vec{b}_1 in the $D \times H$ plane (diagonal state: $D=H+V$) with $\vec{a}_1=D$ and \vec{b}_1 at an angle φ with \vec{a}_1 , \vec{a}_2 and \vec{b}_2 in the $H \times L$ plane ($L=H+iV$) with $\vec{a}_2=H$ and \vec{b}_2 at an angle φ with \vec{a}_2 , and $\vec{b}_3=\vec{a}_2$. To construct these settings, a half-wave plate and a PBS are used in series (as the polarization analyzer) to implement the linear polarization analysis of the signal (idler) photon. In addition, a quarter-wave plate (with 0° rotation) is inserted before the polarization analyzer in the idler beam path when the analysis on the elliptical polarization of the photon is needed. (The quarter-wave plate provides a unitary rotation to flip the plane $D \times H$ into the plane $L \times H$ in the Poincaré sphere.) Because our fiber-based source simultaneously outputs singlet states at multiple wavelengths [13] in a single spatial mode, we are able to easily study Bell's inequality and the Leggett-type NLHV inequality at

different pairs of signal and idler wavelengths by simply translating our wavelength selecting slits. The two pairs of wavelengths measured in this work (see Table I) were chosen because their wavelengths lie in a spectral band that simultaneously allows sufficiently large coincidence rates and coincidence-to-accidental ratios [12].

With a two-photon coincidence rate of 3.5 kHz and single rates of 80 kHz for two sets of signal-idler wavelength pairs, visibilities of the singlet state Ψ^- are measured greater than 97% in H-V, A-D, and L-R bases (see Table I). As shown in Fig. 2, the violation of the Leggett-type NLHV inequality and the violation of Bell's inequality (in the CHSH form)

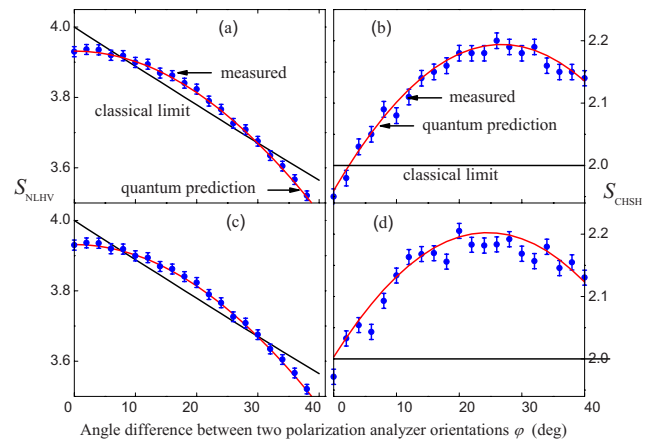


FIG. 2. (Color online) Measured values (blue circles), the quantum prediction (red line), and the classical limit (black line) of S_{NLHV} [(a) and (c)] and S_{CHSH} [(b) and (d)] as a function of φ at two pairs of wavelengths: $\lambda_{\text{signal}}=689$ nm, $\lambda_{\text{idler}}=800$ nm [(a) and (b)], and $\lambda_{\text{signal}}=685$ nm, $\lambda_{\text{idler}}=805$ nm [(c) and (d)].

occur for a number of polarization analyzer settings. At $\varphi = 20^\circ$, we obtained the violation of Leggett-type NLHV inequality by $>3\sigma$ and the violation of Bell's inequality by $>14\sigma$ with the numerical values given in Table I.

Our two independent sets of measurements violate both Bell's inequality and the Leggett type of inequality, thus excluding LHV theories as well as a certain class of NLHV theories. This study also demonstrates that our single-mode, fiber-based source is useful not only for quantum communication applications, but also for investigations into fundamental problems in quantum mechanics.

Note added. Recently, we were made aware of two separate measurements of the violation of a Leggett-type NLHV inequality without the rotational symmetry assumption using a parametric-down-conversion source [14].

This work has been supported in part by the Disruptive Technology Office (DTO) entangled photon source program and the Multidisciplinary University Research Initiative Center for Photonic Quantum Information Systems (Army Research Office/DTO Program No. DAAD19-03-1-0199). M.D.E. acknowledges support from the National Research Council.

-
- [1] E. Schrödinger, *Naturwiss.* **23**, 807 (1935); **23**, 823 (1935); **23**, 844 (1935); J. D. Trimmer, *Proc. Am. Philos. Soc.* **124**, 323 (1980).
- [2] Letter from A. Einstein to M. Born, March 3, 1947, in A. Einstein and M. Born, *The Born-Einstein Letters* (Walker, New York, 1971).
- [3] A. Einstein, B. Podolsky, and N. Rosen, *Phys. Rev.* **47**, 777 (1935).
- [4] J. S. Bell, *Physics* (Long Island City, N.Y.) **1**, 195 (1964).
- [5] J. F. Clauser, M. A. Horne, A. Shimony, and R. A. Holt, *Phys. Rev. Lett.* **23**, 880 (1969); J. F. Clauser and M. A. Horne, *Phys. Rev. D* **10**, 526 (1974).
- [6] A. Zeilinger, *Rev. Mod. Phys.* **71**, S288 (1999); A. Aspect, *Nature* (London) **398**, 189 (1999); P. Grangier, *ibid.* **409**, 774 (2001); M. A. Rowe *et al.*, *ibid.* **409**, 791 (2001).
- [7] A. Leggett, *Found. Phys.* **33**, 1469 (2003).
- [8] S. Gröblacher *et al.*, *Nature* (London) **446**, 871 (2007).
- [9] P. G. Kwiat, E. Waks, A. G. White, I. Appelbaum, and P. H. Eberhard, *Phys. Rev. A* **60**, R773 (1999); J. Altepeter, E. Jeffrey, and P. G. Kwiat, *Opt. Express* **13**, 8951 (2005).
- [10] C. Kurtsiefer, M. Oberparleiter, and H. Weinfurter, *Phys. Rev. A* **64**, 023802 (2001).
- [11] T. Kim, M. Fiorentino, and F. N. C. Wong, *Phys. Rev. A* **73**, 012316 (2006).
- [12] J. Fan and A. Migdall, *Opt. Express* **15**, 2915 (2007).
- [13] J. Fan, M. D. Eisaman, and A. Migdall, *Phys. Rev. A* **76**, 043836 (2007), *Opt. Express* **15**, 18339 (2007).
- [14] T. Paterek, A. Fedrizzi, S. Gröblacher, T. Jennewein, M. Zukowski, M. Aspelmeyer, and A. Zeilinger, *Phys. Rev. Lett.* **99**, 210406 (2007); C. Branciard, A. Ling, N. Gisin, C. Kurtsiefer, A. Lamas-Linares, and A. Scarani, *ibid.* **99**, 210407 (2007).